P-ISSN 2586-9000
E-ISSN 2586-9027
Homepage : https://tci-thaijo.org/index.php/SciTechAsia
Science & Technology Asia
Vol.24 No.1 January - March 2019
Page: [41-53]
Original research article

# Energy and Exergy Analysis of Low-Cooling in Building by using Light-Vent Pipe

Dittha Nonthiworawong[1], Phadungsak Rattanadecho[2] and Ratthasak Prommas[3,*]

[1]Rattanakosin College for Sustainable Energy and Environment,
Rajamangala University of Technology Rattanakosin, Nakhon Pathom, 73170, Thailand.
[2]Center of Excellence in Electromagnetic Energy Utilization in Engineering,
Department of Mechanical Engineering, Faculty of Engineering,
Thammasat University, Pathum Thani 12120, Thailand.
[3]Department of Mechanical Engineering, Faculty of Engineering,
Rajamangala University of Technology Rattanakosin, Nakhon Pathom, 73170, Thailand.

Received 8 March 2018; Received in revised form 7 May 2018
Accepted 5 June 2018; Available online 8 February 2019

## ABSTRACT

This study conducts the energy and exergy analysis of a light-vent pipe which is integrated into attic space. The roof is a shed roof with 30 degrees of inclination angle. The LVP is manufactured from an aluminum sheet with a translucent flat cover and is 0.15 m in diameter. The results show that the test house integrated with the LVP could well transfer heat accumulated in attic space by natural ventilation through the LVP. The natural daylight has an influent to the air mass flow rate corresponding to energy and exergy efficiency. The total energy and exergy efficiencies were 37-67% and 12.3-33%, respectively. In addition, the ceiling heat gain and exergy heat gain performed that, the requirement of space cooling of the house with LVP lower than that the reference house.

**Keywords:** Light-vent pipe; Energy and exergy; Ceiling heat gain; Daylight

## 1. Introduction

Energy and exergy analysis in buildings is one of the most promising solutions for energy conservation. The cooling load of the rooms is dependent on the internal and external heat loads. One of the important heat loads is the solar energy, which is also known as an external heat load. Several techniques were considered and applied to the building envelope, viz. ventilation, insulations and materials. The classical technique is the solar chimney concept as applied to the ventilated roof [1], ventilated wall [2] and ventilated attic [3]. The significant building components are roof and wall; named Roof Solar Collector

*Corresponding author: ratthasak.pro@rmutr.ac.th doi: 10.14456/scitechasia.2019.5

(RSC) [1, 4], Bio-Climatic Roof (BCR) [5], Roof solar collector with radiant barrier (RSC-RB) [6], PV Roof Solar Collector (PV-RSC) [7] and Thai Modern Facade wall (TMF) [8-9]. Ref. [4] investigated the field measurement to evaluate the performance of a solar roof collector. A small house of 25 $m^3$ was designed and built using common materials with two units of RSC integrated on the roof. Each RSC has 1.5 $m^2$ surface area. The tilt angle was fixed at 25°. Four configurations for the inlet and outlet opening vents of RSC were considered. The experimental results showed that a large air gap and large and equal size of opening vents provided a high ventilation rate. In Waewsak et al. [5], the BCR consists of a combination of CPAC Monier tile and acrylic transparent tile at the upper plane and the lower plane combined with gypsum board with aluminum foil and translucent sheet at the room space side. The experiments were carried out in winter and summer. The results showed that the BCR could reduce the roof heat gain and provide sufficient natural lighting in the room. The BCR provided the indoor illuminance of about 300 and 140 in summer and winter, respectively; and also provided air change of about 13-14 and 5-7 ACH in summer and winter, respectively [6].

They have presented the performance in terms of temperature, induced natural ventilation, amount of air change, and indoor illuminance; these parameters confirmed the thermal and daylighting performance. However, they reported only energy transfer (First law of Thermodynamics), which is not adequate for the system analysis. The exergy analysis (Second law of Thermodynamics) can explain the quality change of energy.

The exergy analysis and parametric study of concentrating type solar collector has been studied [10-11]; the exergy performance was made using hourly solar radiation. The exergy output was optimized with respect to the fluid inlet temperature. Energy and exergy analysis of a photovoltaic-thermal collector was investigated [12]. Based on experimental and numerical models, a study of the appropriateness of a glass cover on a thermosiphon-base water heating PV/T system was carried out. The influences of six selected operating parameters were evaluated. Meanwhile, Dubey et al. [13] investigated the energy and exergy analysis of PV/T air collectors connected in series. The performance of the collector was evaluated by considering two different cases: in Case I air collector was fully covered by PV modules and air flowed above the absorber plate; in Case II air collector was fully covered by PV modules and air flowed below the absorber plate. The experiments presented the detailed analysis of energy, exergy and electrical energy by varying the number of collector and air velocity considering four weather conditions. Energy and exergy analysis of different Trombe walls [14] was investigated by Duan et al. The performance of two different Trombe walls was examined: one with the absorber plate pasted on the thermal storage wall (Type I) and one with the absorber plate placed between the glass cover and the thermal storage wall (Type II). The energy and efficiencies of the Trombe wall were evaluated for various air channel depth, solar radiation and the emissivities of the glass cover. Meanwhile, Corasaniti et al. [15] investigated the numerical simulation of modified Trombe-Michel Walls with exergy and energy analysis. Three configurations of modified Trombe-Michel Wall (TMW) were investigated: with sharp edges, with rounded edges, and with the guided flow. Heat transfer and exergy loss on the oscillating circular pipe were studied by Gul and Akpinar [16]. The parameters for this study were chosen as a Reynolds number from 5000 to 20,000 at the oscillating frequency with 10 and 20 Hz. The exergy loss of the horizontal concentric

micro-fin tube heat exchanger was investigated by Naphon [17]. The results showed that the relevant parameters had significant effect on the entropy generation, entropy generation number and exergy loss. The predicted results obtained from the model were validated by comparing with the present measured data.

Energy and exergy analysis in the building was proposed by [18-21]. Ref. [18] presented the energy and exergy analyses of space heating in buildings; this study proposed the calculations such as heat losses and gain be taken according to the Turkish Standard Institution. In the analysis, heating load was taken into account but the cooling load was neglected, and the calculations presented used a steady state condition. The analysis was applied to an office with a volume of 720 $m^3$ and a net floor area of 240 $m^2$; indoor and exterior air temperatures were 20°C and 0°C, respectively. Ref. [19] investigated the exergy analysis by variable air volume systems for an office building. In this study, energy and exergy analysis was utilized for evaluating two types of VAV systems operating in a large office building. The COP of the system already showed a very low performance according to the First law of Thermodynamics; the exergy efficiency showed an alarmingly low value only 2-3% of potential work that could be developed by using another energy sources. Thermodynamic analysis of a building using the exergy analysis method was performed by Yucer and Hepbasli [20]; this study dealt with exergetic assessment of an educational building heated by a conventional boiler in a heating center. The heat loss calculations were made using both energy and exergy analysis methods. The energy and exergy flow between the stages were obtained using a pre-design tool for an optimized building design.

This paper expresses the energy and exergy analyses (First and Second laws of Thermodynamics) of a light-vent pipe. The indicator evaluations are energy and exergy efficiencies of LVP.

## 2. Energy and exergy analysis

Generally, the first and second laws of thermodynamics are applied to estimate the first and second law efficiencies. Based on the experimental results, the energy and exergy efficiencies of light-vent pipe (LVP) are calculated.

### 2.1 Energy analysis

In the entire efficiency analysis of the LVP, an important step is to estimate the energy flow through the LVP, which is induced by natural flow. The first law of thermodynamics is defined under a steady state open system. The energy flow can be calculated by: Eq.(2.1)

$$\dot{Q}_f = \dot{m} C_p (T_o - T_i) \qquad (2.1)$$

Where $\dot{Q}_f$ is the energy flow through the LVP; $\dot{m}$ is the air mass flow rate, $C_p$ is the specific heat at constant pressure, $T_o$ is the outlet air flow temperature, and $T_i$ is the inlet air flow temperature.

In this system, the daylight could be converted to energy in terms of power as given by Eq.(2.2)

$$P_{dl} = \frac{E_{dl} A_{dl}}{\eta} \qquad (2.2)$$

Where $P_{dl}$ is the power from daylight; $E_{dl}$ is the illuminance, $A_{dl}$ is the arear, and $\eta$ is the efficacy of lumens per watt.

The heat transfer from the attic space transferred to the LVP $\dot{Q}_{attic-LVP}$ surface can be estimated by Eq.(2.3)

$$\dot{Q}_{attic-LVP} = \bar{h} A_p (T_{attic} - T_s) \qquad (2.3)$$

Where $Q_{attic-LVP}$ is heat transfer from the attic to the LVP surface, $\bar{h}$ is the heat

transfer coefficient, $A_p$ is the external LVP surface area, $(A_p = \pi DL)$, $T_{attic}$ is the attic temperature, and $T_s$ is the pipe surface temperature.

The heat transfer coefficient can be evaluated from the empirical correlations external free convection flows; the correlations are suitable for most calculations as follows:

$$\overline{Nu}_L = \frac{\overline{h}L}{k} \tag{2.4}$$

$$\overline{Nu}_L = \left[ 0.825 + \frac{0.387 Ra_L^{1/6}}{\left[1 + (0.492/\mathrm{Pr})^{9/16}\right]^{8/27}} \right]^2 \tag{2.5}$$

$$Ra_L = \frac{g\beta(T_{attic} - T_s)L^3}{\nu\alpha} \tag{2.6}$$

The foregoing results may be applied to vertical cylinders of height L, if the boundary layer thickness is much less than the cylinder diameter ($D/L \geq 35/Gr_L^{1/4}$), [22].

The energy efficiency of LVP may be calculated by Eq.(2.7)

$$\eta = \frac{\dot{Q}_f + P_{dl}}{I_T A_{dl} + Q_{attic-LVP}} \tag{2.7}$$

Where $\eta$ is thermal efficiency of LVP and $I_T$ is solar radiation.

**2.2 Exergy analysis**

The exergy analysis is based on the second law of thermodynamics. Under steady state conditions, the exergy equation can be written as equation (2.8), which includes the total exergy inflow, exergy outflow and exergy destruction of the system:

$$\sum \dot{E}x_i = \sum \dot{E}x_o + \sum \dot{E}x_{dest} \tag{2.8}$$

Where $\sum \dot{E}x_i$ is the rate of total exergy inflow; $\sum \dot{E}x_o$ is the rate of total exergy outflow and $\sum \dot{E}x_{dest}$ is the rate of exergy destruction of the system.

The total exergy inflow $\sum \dot{E}x_i$ to the LVP can be calculated as:

$$\sum \dot{E}x_i = \dot{E}x_{i,air} + \dot{E}x_{i,abs-surf} + Ex_{sun,daylight} \tag{2.9}$$

The naturally flowed of the thermal exergy inflow from the air flow through the LVP can be defined by Eq.(2.10)

$$\dot{E}x_{i,air} = \dot{m}c_p \left[ \left(T_{f,i} - T_{amb}\right) - T_{amb} \ln\left(\frac{T_{f,i}}{T_{amb}}\right) \right] \tag{2.10}$$

The exergy inflow to the PVL from the attic is given by Eq.(2.11)

$$\dot{E}x_{i,attic-LVP} = \left(1 - \frac{T_{amb}}{T_{attic}}\right) Q_{attic-LVP} \tag{2.11}$$

Where $\dot{E}x_{i,attic-LVP}$ is the exergy inflow from the attic to LVP surface, given by Eq. (2.11), $\dot{E}x_{i,air}$ is the thermal exergy at inlet air flow to the LVP, given by Eq. (2.12), $T_{amb}$ is the ambient temperature and $T_{attic}$ is the attic temperature.

The exergy from illuminance can be determined as

$$\dot{E}x_{i,sun,daylight} = I_T A_{dl} \left( 1 - \frac{4}{3}\left(\frac{T_{amb}}{T_{sunc}}\right) + \frac{1}{3}\left(\frac{T_{amb}}{T_{sun}}\right)^4 \right) \tag{2.12}$$

Where $\dot{E}x_{i,sun,daylight}$ is the exergy from illuminance; $I_T$ is the solar radiation, $A_{dl}$ is the cross-section area, and $T_{sun}$ is the sun temperature (5777 K, [23]).

The rate of exergy outflow is defined by Eq. (2.13)

$$\sum \dot{E}x_o = \dot{E}x_{o,air} + Ex_{o,dl} \quad (2.13)$$

Where $\dot{E}x_{o,air}$ is the rate of thermal exergy outflow from the air flow, given by Eq. (2.14),

$$\dot{E}x_{o,air} = \dot{m}c_p\left[\left(T_{f,o} - T_{amb}\right) - T_{amb}\ln\left(\frac{T_{f,o}}{T_{amb}}\right)\right] \quad (2.14)$$

The exergy from daylight is given by Eq.(2.15)

$$P_{dl} = \frac{E_{dl}A_{dl}}{\eta} \quad (2.15)$$

The exergy efficiency of LVP can be calculated as Eq. (2.16)

$$\varepsilon = \frac{\dot{E}x_{o,air} + Ex_{o,dl}}{\dot{E}x_{i,air} + \dot{E}x_{i,abs-surf} + Ex_{sun,daylight}} \quad (2.16)$$

Where $\varepsilon$ is the exergy efficiency.

### 2.3 Heat flow rate

After the mass flow rate is calculated, the heat flow rate due to ventilation must be calculated.

The heat flow rate due to ventilation of air between the interior of a test house and the outside is given by eq. (2.17):

$$\dot{Q}_{vent} = \dot{m}C_p(T_o - T_i) = \left(\rho C_p \frac{NV}{3600}\right)(T_o - T_i) \quad (2.17)$$

Where $\dot{Q}_{vent}$ is the heat flow rate due to ventilation; $N$ is the amount of air change, and $V$ is the volume of the model house.

## 3. Experimental description

A schematic of two small houses, which were designed and built for this study, is shown in Fig. 1. They are located in Salaya, Puthamonthon, Nakhonpathom, Thailand. The main structure was built from steel. Other construction materials consisted of corrugated metal sheets for the roof and walls, gypsum boards for the ceiling, and a reinforced concrete floor. Each house has an identical floor area of about 1 $m^2$ and the height from floor to ceiling is 2.0 m. The roof is a shed roof (3.4 $m^2$/ house) with 30 degrees of angle. The reference house was thatched with the corrugated metal sheet, while the test house was thatched with the same material and a light-vent pipe was installed. The LVP used in this work has been designed to consist of a vertical section and an inclined section joined with an elbow (equal roof inclination angle); the vertical and inclined sections have lengths of 40 cm and 80 cm, respectively. Each pipe diameter is 15 cm. The natural ventilation applied in the pipe, the flow rate through the LVP is satisfactory improving beneficial of the system.

The ventilation pattern is the cross ventilation: the air flows first through the door into the room space, then to the inlet of the light-vent pipe at the ceiling, and exits at the outlet of the LVP as shown in Fig. 2.

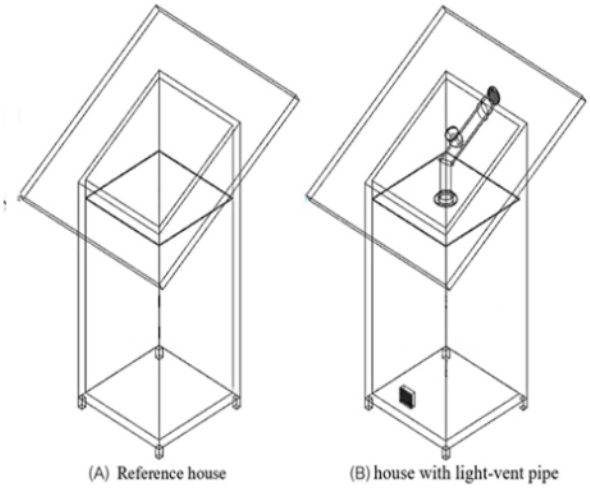


**Fig. 1.** Photograph of the houses in the experiment.

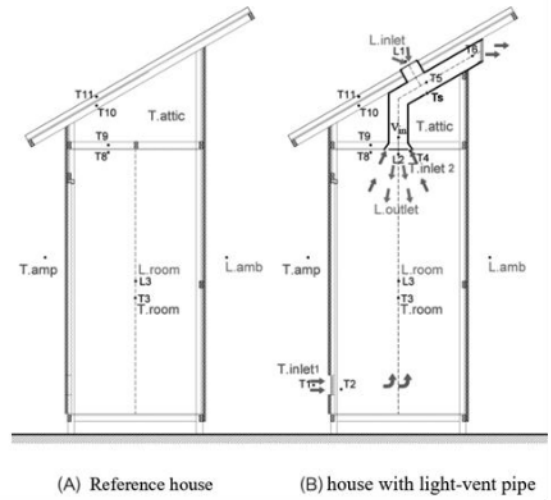


**Fig. 2.** The measuring positions of temperatures, illuminance and air velocity.

Thermocouple type K has a range 0-1250°C, and accuracy ±0.5°C. The heat flux sensor, the Omega HFs-3, which has a range 1-1400 W/m$^2$, measured the ceiling heat gain. A pyranometer (Kipp&Zonen), Model: CMP11 has a range of 310-2800 μm, and the uncertainty < 2% connected to a data logger named Hioki: Model 8422-52 with accuracy of ±0.8%. The illuminance was measured by using lux meter (Testo: Model 545, accuracy ±5%). The hot wire anemometer, KIMO VT-100, which measured the air velocity, has a range of 0-50 m/s and error of ±0.5%. The data interval was recorded every 30 minutes from 10:00 a.m. to 3:00 p.m. The houses have installed thermocouples to measure the temperatures at the roof, attic, ceiling, and room as shown in Fig. 2. Further thermocouples were used to measure the inlet and outlet air temperatures, and ambient temperature. Heat flux was measured at the ceiling (room side). Air velocity was measured at the center of the pipe. The indoor illuminance and outdoor illuminance were measured on the work plane and horizontal plane, respectively.

The uncertainty analysis is important to evaluate the accuracy of the results from the experiments. Without a measure, it is impossible to judge the appropriateness of the value as a basis for making decisions. The uncertainties arising in calculating a result ($w_R$) due to several independent variables are presented in [25]

$$w_R = \left[ \left( \frac{\partial R}{\partial x_1} w_1 \right)^2 + \left( \frac{\partial R}{\partial x_2} w_2 \right)^2 + \cdots + \left( \frac{\partial R}{\partial x_n} w_n \right)^2 \right]^{1/2} \quad (3.1)$$

Where the result R is a function in terms of its independent variables as $x_1, x_2, x_3, \ldots\ldots x_n$, thus $R = R(x_1, x_2, x_3, \ldots, x_n)$, $w_R$ is the uncertainty of the result, and $w_1, w_2, \ldots, w_n$ are the uncertainties in the independent variables.

In this study, the temperature and air mass flow rate were measured with appropriate instruments as explained previously. Uncertainties for each measured and calculated parameter are calculated using Eq (3.1).

The total uncertainties of the measurements are evaluated to be ±2.3% for air mass flow rate, ±2.5% for heat flow and ±2.0% for temperature.

## 4. Results and Discussion

### 4.1 Ambient condition and temperatures

The experiment investigated the thermal performance of a light-vent pipe (LVP), which was integrated into an attic space to decrease the energy and exergy needs in an interior room. The solar radiation is the most significant factor to produce heat gain in the building; and the ambient temperature is also important to analysis the energy and exergy.

The experimental data were collected during February to April 2017. The most beneficial day was selected to obtain the ambient condition of the experiment as shown in Fig. 3; there was a clear sky when solar radiation was high, and wind velocity was very low. During the test period, the maximum solar radiation on the tile surface was 700 W/m$^2$ and the average

ambient temperature was 35°C. They gradually increased from 10:00 to 12:00 and decreased from 12:00 to 15:00.

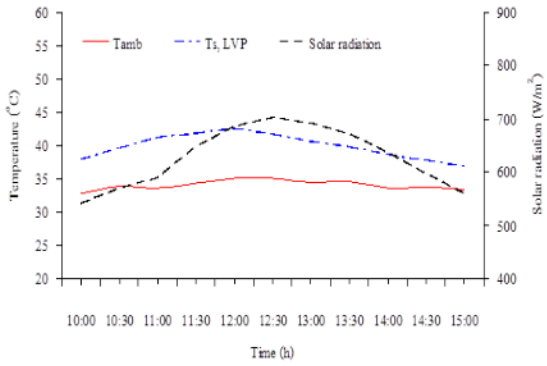


**Fig. 3.** Hourly variation of solar radiation and ambient temperature

Meanwhile, Fig. 3 illustrates the situation of the LVP surface temperatures. It was observed that there was a gradual rise in the LVP surface temperature from 10:00 to 12:00 as solar radiation increased and then a gradual drop of LVP surface temperature from 12:00 to 15:00 as solar radiation decreased. It was apparent that the LVP surface had been affected by solar radiation.

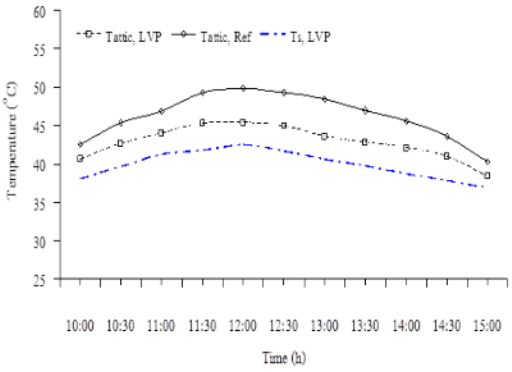


**Fig. 4.** Attic temperature and LVP surface temperature.

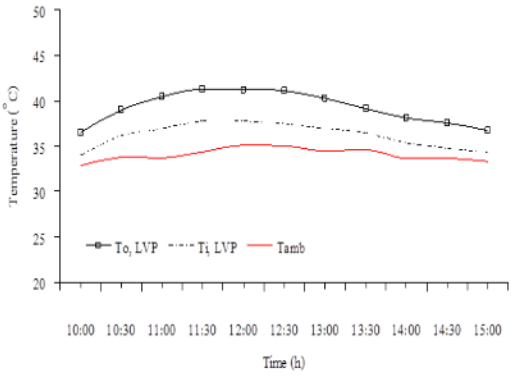


**Fig. 5.** Inlet and outlet airflow temperature and ambient temperature.

In Fig. 4 also illustrates the LVP surface temperature and attic temperatures of the reference house and the house with integrated LVP. It was apparent that the attic temperature of the reference house was higher than the house with LVP throughout the day. Subsequently, Fig 5 illustrates the inlet and outlet air flow temperatures of the LVP. To aid in understanding, Fig 4 helps to explain the situation of the airflow temperature. It was observed that the LVP surface absorbed some heat in the attic space, and transferred it to the environment by natural air flow.

### 4.2 Analysis of mass flow rate for LVP

In order to estimate the performance of the LVP, the data analysis is presented in term of energy and exergy, and also energy and exergy efficiency. Firstly, the air mass flow rate must be presented to be able to understand the relationship between air mass flow rate and air temperature; the fact that the density of air as a function of temperature.

The mechanism of mass flow rate and heat transfer through the LVP can be described by the theoretical model.

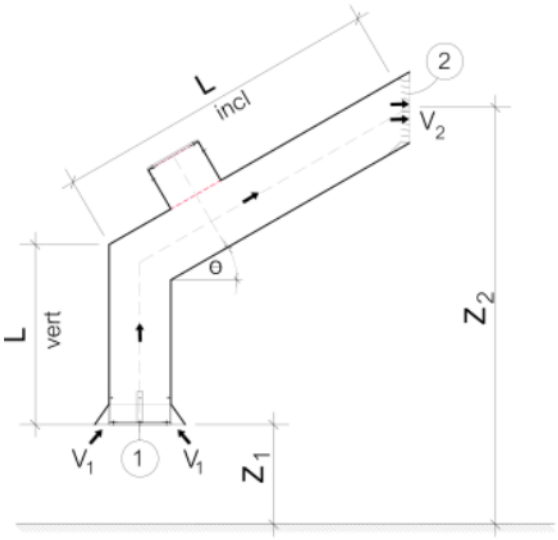


**Fig. 6.** Section the inlet and outlet air flow model.

The LVP with hot air that accumulates in the attic space performs like an air to air heat exchanger, while the heated air flows up through the LVP by buoyancy force. The LVP is located at one vent on the ceiling and at one vent at the edge of the roof. The mass flow rate through the LVP depends on the temperature difference between the inlet and outlet airflow temperature, inlet and outlet pressure losses, and wall friction factor.

In this study, the natural flow for the LVP system under steady state is derived by applying Bernoulli's equation from inlet to outlet of the LVP as shown in Fig. 6. The inlet and outlet area are not equal to the cross section area.

$$P_1+\frac{\rho_1 v_1^2}{2}+\rho_1 g Z_1=P_2+\frac{\rho_2 v_2^2}{2}+\rho_2 g Z_2+f\frac{L}{D}\frac{\rho v^2}{2}\bigg|_{vert}+f\frac{L}{D}\frac{\rho v^2}{2}\bigg|_{incl}$$

$$+K_1\frac{\rho_1 v_1^2}{2}+K_{120}\frac{\rho v^2}{2}+K_2\frac{\rho_2 v_2^2}{2} \quad (4.1)$$

$$\dot{m}=\rho_1 A_1 v_1=\rho_2 A_2 v_2=\rho A_p v \quad (4.2)$$

the relationship between temperature and density are given by:

$$\rho_T=\rho\beta T \quad (4.3)$$

Rearranging and solving equations (4.1), (4.2) and (4.3) obtains:

$$\beta g(L_{vert}+L_{incl}\cdot\sin\theta)(T_o-T_i)=\beta T_1(K_1-1)\frac{v^2}{2}\left(\frac{A_p}{A_1}\right)^2+$$

$$\beta T_2(K_2+1)\frac{v^2}{2}\left(\frac{A_p}{A_2}\right)^2+K_{120}\frac{v^2}{2}+\left[f\frac{L}{D}\bigg|_{vert}+f\frac{L}{D}\bigg|_{incl}\right]\frac{v^2}{2} \quad (4.4)$$

The expression for the air mass flowrate is obtained by rearranging equation (4.4) to yield:

$$\dot{m}=\left(\frac{2\beta g(L_{vert}+L_{incl}\cdot\sin\theta)(\rho A_p)^2(T_o-T_i)}{\left[\beta T_i(K_i-1)\left(\frac{A_p}{A_i}\right)^2+\beta T_o(K_o+1)\left(\frac{A_p}{A_o}\right)^2+K_{30}+\left[f\frac{L}{D}\bigg|_{vert}+f\frac{L}{D}\bigg|_{incl}\right]\right]}\right)^{\frac{1}{2}} \quad (4.5)$$

Where  is the mass flow rate, f is friction coefficient (f=0.05 [22]), $K_i$ is an inlet pressure loss ($K_i$ =3 [24]), $K_o$ is outlet pressure losses ($K_o$ = 3, [24]), $L_{vert}$ is the pipe length (vertical), $L_{incl}$ is pipe length (inclined), D is the diameter of the circular pipe,  is internal surface area of the pipe,  is thermal expansion coefficient,  is inlet air flow temperature,  is outlet air flow temperature.

Equation (4.5) is applied for calculation of air mass flow rate through the LVP by natural flow. Fig. 7 compares the measured and calculated air mass flow rate through the LVP and shows that they were had similar trends throughout the day. This indicates that this model is suitable for this system.

Fig. 5 and Fig. 8 illustrate the measured air velocity and air mass flow rate. It was observed that as the air flow temperatures were increasing the air velocity and air mass flow rate were also increasing in a similar way.

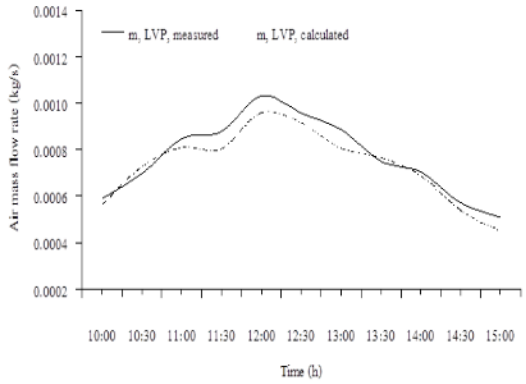


**Fig. 7.** Hourly variation of air mass flow rate (measured and calculated).

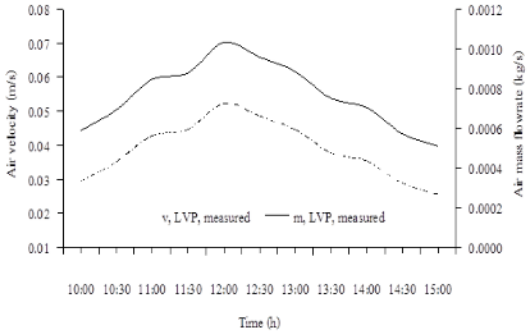


**Fig. 8.** Air mass flow rate and air velocity.

### 4.3 Energy and Exergy analysis

In order to evaluate the energy and exergy efficiency of the LVP; on the basis of the experimental data, viz. air flow temperatures, LVP surface temperature, [26-27] etc. As mentioned earlier, the experimental data are solved and described. As shown in Fig. 9, the amount of measured indoor illuminance on the work plane and the outdoor illuminance on horizontal plane range from 40 to 90 kLx and from 230 to 320 Lx, respectively. It was apparent that the indoor illuminance is close to the standard indoor illuminance (300 Lx for working plane [9])

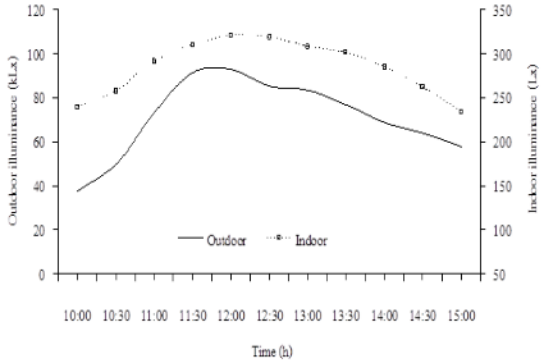


**Fig. 9.** Indoor and outdoor illuminances.

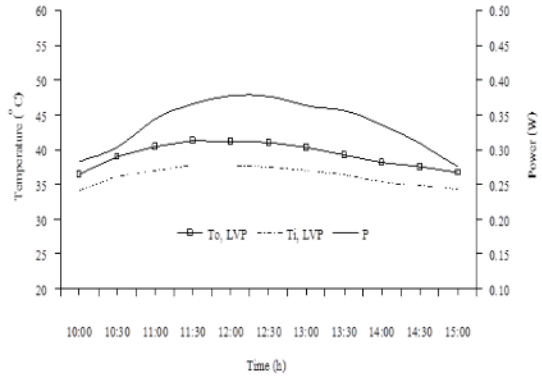


**Fig. 10.** Air flow temperature and power from natural daylight.

Besides this, there were other relationships; the difference between inlet and outlet air flow temperatures and power from natural daylight. Earlier in section 2, the power of natural daylight was formulated as $P_{dl} = E_{dl} A_{dl} / \eta$. Where $P_{dl}$ is the power from daylight; $E_{dl}$ is the illuminance, $A_{dl}$ is the area, and $\eta$ is the efficacy of lumens per watt. Fig. 10 shows the air flow temperature and power from natural daylight. It was observed that, while the air flow temperature difference was increasing, the calculated power from natural daylight was increasing.

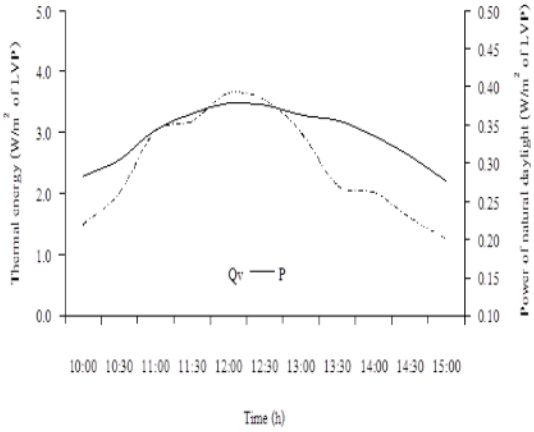


**Fig. 11.** Thermal energy and power from natural daylight per unit cross-section area of LVP.

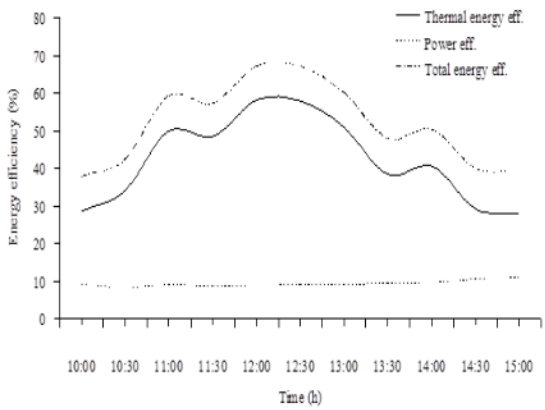


**Fig. 12.** Thermal energy, power energy from daylight and total energy efficiency of LVP.

Fig. 11 shows the thermal energy and power from natural daylight per cross-section area of LVP. The cross-section area is about 0.0177 $m^2$, which is small but appropriate for this experiment. It was apparent that the thermal energy flows through the LVP range of about 1.5 to 4 W/ $m^2$ of LVP cross-section area, and also the power from natural daylight ranged from 0.25 to 0.38 W/ $m^2$ of the LVP cross-section area. To aid in understanding, Fig. 2 helps to explain the situation of Fig. 11. In Fig. 2, it was observed that the attic temperature of the reference house was higher than the house with LVP due to some heat in the attic space being absorbed by the LVP surface and some heat being transferred to the airflow through the LVP; some amount of heat was stored in the LVP. For this reason, the ceiling heat gain was decreased, corresponding to decreased energy and exergy needs in the house with LVP.

Fig. 12 shows the hourly variations of thermal energy, power from daylight and total efficiencies. It was observed that thermal energy, power and total efficiencies ranged between 28-58%, 8.2-11%, and 37-67%, respectively. However, the total efficiency of the LVP depended on the heat accumulated in attic space and the dimension of LVP, viz. diameter, length, etc.

The exergy inflow, exergy outflow and exergy efficiency have been analyzed and presented in this section. Fig. 13 shows the exergy inflow and exergy outflow of the LVP. It can be seen that the exergy inflow was gradually increasing from 10:00 to 12:00 and decreasing from 12:00 to 15:00; the minimum and maximum inflow were 9 and 12 W/$m^2$ cross-sectional area of LVP, respectively. Meanwhile, the exergy outflow ranged between 0.3-0.45 W/$m^2$ cross-sectional area of LVP.

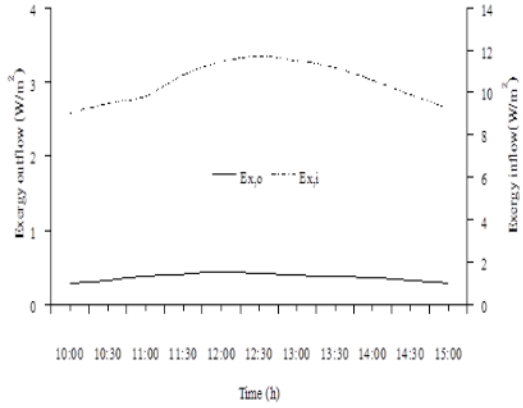


**Fig. 13** Hourly variation of exergy inflow and exergy outflow.

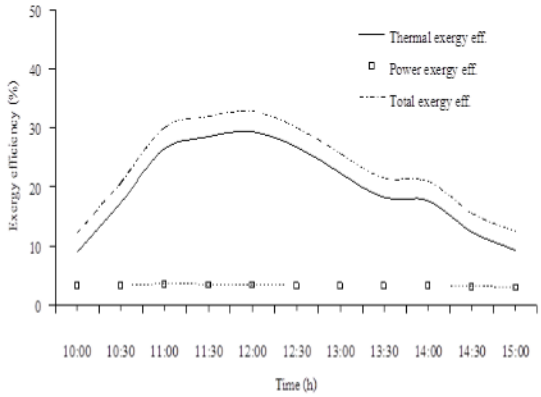


**Fig. 14.** Thermal exergy, power exergy from daylight and total exergy efficiency of LVP.

Fig. 14 shows the hourly variation of exergy efficiency of LVP. There are variations of thermal energy, power from daylight and total exergy efficiencies between 9.3-29.5%, 2.9-3.5% and 12.3-33%, respectively. To better understand the energy and exergy needs for room space, the measured ceiling heat gain and exergy ceiling heat gain were described.

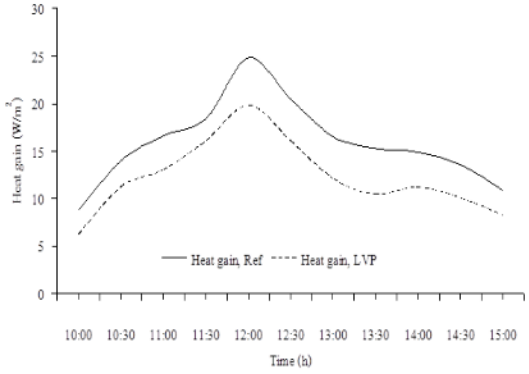


**Fig. 15.** Hourly variation of ceiling heat gain.

To obtain experimentally measured data, the heat flux sensor was used to measure at the center of the ceiling (room side). It was observed that the house with the integrated LVP in the attic space could decrease heat gain through the ceiling better than that the reference house.

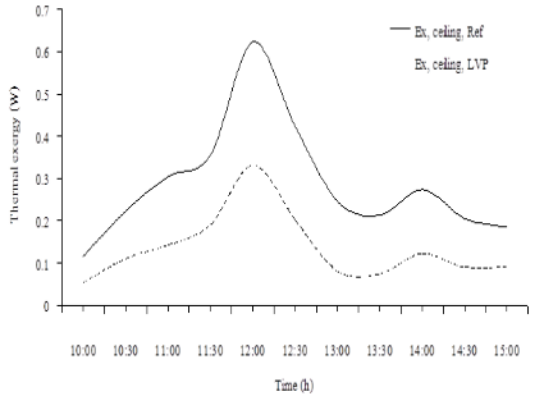


**Fig. 16.** Hourly variation of exergy ceiling heat gain.

The minimum and maximum heat gain reductions were 2.5 and 5 W/m$^2$ per unit of LVP, respectively as shown in Fig. 15. Furthermore, the exergy ceiling heat gain of the reference house and the house with LVP were 0.1 and 0.2 W/m$^2$ per unit of LVP, respectively, as shown in Fig. 16. These results indicate that the LVP could provide energy and exergy needs in the room space.

## 5. Conclusion

In this study, energy and exergy analysis was used to evaluate the energy and exergy efficiency of the LVP. Although the energy efficiency shows good efficiency, the exergy efficiency shows the appropriate value of potential work.

The measured ceiling heat gain is considered to help explain the efficiency calculation. It confirmed that the LVP could decrease the external load through the roof corresponding to reduced energy and exergy needs in space room.

Additional conclusions are as follows:

- The power from natural daylight increased by increasing indoor illuminance, while the temperature difference between inlet and outlet air temperatures of LVP shows variations with power from natural daylight.

- The energy and exergy efficiencies increased with increasing mass flowrate.
- There is good agreement between measured and calculated values of mass flow rate.

## Acknowledgement

The authors would like to thank Rattanakosin College for Sustainable Energy and Environment (RCSEE), Rajamangala University of Technology Rattanakosin (RMUTR) for providing support for this research.

## References

[1] Khedari J, Hirunlabh J, Bunnag T. Experimental study of a roof solar collector towards the natural ventilation of new houses, Energy and Buildings, 1997;26: 159-164.

[2] Khedari J, Pongsatirat C, Puangsombut W, Hirunlabh J. Experimental performance of a partially-glazed modified Trombe wall, Int. J. Ambient Energy, 2005;26(1):27-36.

[3] Juengpimonyanon K, Puangsombut W, Ananacha T. Field investigation on thermal performance of tile ventilator, Applied Mechanics and Materials, 2014;619:73-77.

[4] Khedari J, Mansirisub W, Chaima S, Hirunlabh J. Field measurements of performance of roof solar collector, Energy and Buildings, 2000;31:171-178.

[5] Waewsak J, Hirunlabh J, Khedari J, Shin UC. Performance evaluation of the BSRC multi-purpose bio-climatic roof, Building and Environment, 2003;38:1297-1302.

[6] Puangsombut W, Hirunlabh J, Khedari J, Zeghmati B, Win MM. Enhancement of natural ventilation rate and attic heat gain reduction of roof solar collector using radiant barrier, Building and Environment, 2007;42:2218-2226.

[7] Phiraphat S, Prommas R, Puangsombut W. Experimental study of natural ventilation in PV roof solar collector, Int. Comm. Heat Mass Transf., 2017;89:31-38.

[8] Ananacha T, Puangsombut W, Hirunlabh J, Khedari J. Daylighting and thermal performance of Thai modern façade wall, Energy Procedia, 2014;52:271-277.

[9] Ananacha T, Puangsombut W, Hirunlabh J, Khedari J. Field investigation of the thermal performance of a Thai modern façade wall, Int. J. Ventilation, 2014; 12(3):223-233.

[10] Tyagi SK, Wang S, Singhal MK, Kaushik SC, Park SR. Exergy analysis and parametric study of concentrating type solar collector, Int. J. Thermal Sciences, 2007;46:1304-1310.

[11] Ucar A, Inalli M. Thermal and exergy analysis of solar air collectors with passive augmentation techniques, Int. Comm. Heat Mass Transf., 2006;33(10):1281-1290.

[12] Chow TT, Pei G, Fong KF, Lin Z, Chan A. LS, Ji J. Energy and exergy analysis of photovoltaic-thermal collector, Applied Energy, 2009;86:310-316.

[13] Dubey S, Solanki SC, Tiwari A. Energy and exergy analysis of PV/T air collector connected in series, Energy and Buildings, 2009;41:863-870.

[14] Duan S, Jing C, Zhao Z. Energy and exergy analysis of different Trombe walls, Energy and Buildings, 2016;126:517-523.

[15] Corasaniti S, Manni L, Russo F, Gori F. Numerical simulation of modified Trombe-Michel walls with exergy and energy analysis, Int. Comm. Heat Mass Transf., 2017;88:269-276.

[16] Gul H, Akpinar EK. Investigation of heat transfer and exergy loss in oscillating circular pipes, Int. Comm. Heat Mass Transf., 2007;34:93-102.

[17] Naphon P. Study on the exergy loss of the horizontal concentric micro-fin tube heat exchanger, Int. Comm. Heat Mass Transf. 2011;38:229-235.

[18] Yildiz A, Gungor A. Energy and exergy analyses of space heating in buildings, Applied Energy, 2009;86:1939-1948.

[19] Wei Z. Zmeureanu, R., Exergy analysis of variable air volume systems for an office building, Energy Conversion and Management, 2009;50:387-392.

[20] Yucer CT, Hepbasli A. Thermodynamic analysis of a building using exergy analysis method, Energy and Buildings, 2011,43: 536-542

[21] Baldi MG, Leoncini L. Thermal exergy analysis of a building, Energy Procedia, 2014;62:723-732.
[22] Incopera FP, Witt DD. Fundamental of Heat and Mass Transfer, Third Ed., John Wiley & Sons, United State of America, 1981.
[23] Moran MJ. Availability analysis: A guide to efficiency energy use, Prentice-Hall Inc. Englewood Cliffs, 1982.
[24] McQuiston FC, Parker JD. Heating, Ventilating and Air Conditioning Analysis and Design, Fourth Ed. John Wiley & Sons, United State of America, 1994.
[25] Holman JP. Experimental Method for Engineers, sixth ed., McGraw-Hill Co,Singapore, 1994.
[26] Abdulmunem RA, Jalal MJ. Indoor investigation and numerical analysis of PV cells temperature regulation using coupled PCM/Fins, International Journal of Heat and Technology, 2018;36(4):1212-1222.
[27] Kiran KG, Saboor S, Ashok BTPR. Setty. Day lighting and thermal analysis using various double reflective window glasses for green energy buildings, International Journal of Heat and Technology, 2018; 36(3):1121-1129.